Environment International 213 (2026) 110343

Contents lists available at ScienceDirect

Environment International

journal homepage: www.elsevier.com/locate/envint

Full length article

Anthropogenic nitrogen impacts on global $PM_{2.5}$–O_3 co-pollution health burden

Song Liu [a], Xicheng Li [b], Lei Shu [c], Tzung-May Fu [b,d,e], Xin Yang [b,d,e], Lei Zhu [b,d,e,*], Jing Wei [f,*]

[a] Institute of Space Earth Science, Nanjing University, Suzhou 215163, China
[b] School of Environmental Science and Engineering, Southern University of Science and Technology, Shenzhen 518055, China
[c] School of Geographical Sciences, Fujian Normal University, Fuzhou 350117, China
[d] Guangdong Provincial Field Observation and Research Station for Coastal Atmosphere and Climate of the Greater Bay Area, Southern University of Science and Technology, Shenzhen 518055, China
[e] Shenzhen Key Laboratory of Precision Measurement and Early Warning Technology for Urban Environmental Health Risks, School of Environmental Science and Engineering, Southern University of Science and Technology, Shenzhen 518055, China
[f] MEEKL-AERM, College of Environmental Sciences and Engineering, Institute of Tibetan Plateau, and Center for Environment and Health, Peking University, Beijing, China

ARTICLE INFO

Keywords:
$PM_{2.5}$–O_3 health synergy
Anthropogenic nitrogen emissions
Machine learning
Model simulation

ABSTRACT

The growing recognition of the adverse health impacts posed by ambient fine particulate matter ($PM_{2.5}$) and ozone (O_3) has driven global efforts to implement stricter regulations on reactive nitrogen emissions, including nitrogen oxides (NO_x) and ammonia (NH_3). Nevertheless, effective mitigation strategies remain constrained by the gap between precursor emissions and health effects, especially in regions facing compounded $PM_{2.5}$–O_3 pollution. This work models the synergistic health burden from $PM_{2.5}$–O_3 co-exposure and its complex responses to anthropogenic nitrogen emission controls. Our modeling reveals a significant positive interaction between $PM_{2.5}$ and O_3, with co-exposure mortality 24.8% higher than non-interactive additive estimates. NO_x and NH_3 emissions contribute to 20.3% and 19.4% of these deaths, respectively, with relative importance varying across regions and seasons. To mitigate joint $PM_{2.5}$–O_3 health impacts, NO_x reduction is currently more effective than NH_3 control, though sustained benefits require coordinated cuts to both species. Importantly, due to a non-linear emission–health relationship, only aggressive emission reductions can generate proportionally significant health gains, exceeding 20.2% improvements over mild control scenarios. These findings challenge conventional uniform emission control measures and provide a scientific basis for developing dynamic air quality and health management frameworks.

1. Introduction

Exposure to ambient fine particulate matter (aerodynamic diameter ≤ 2.5 μm; $PM_{2.5}$) and ozone (O_3) is associated with adverse health effects on human health, responsible for over 5 million premature deaths annually through both chronic and acute effects (GBD 2019 Risk Factors Collaborators, 2020; GBD 2021 Risk Factors Collaborators, 2024; Liu et al., 2024a). Recent epidemiological evidence indicates a concerning synergistic effect between $PM_{2.5}$ and O_3, with combined exposure exhibiting amplified mortality risk than the sum of individual exposure (C. Liu et al., 2023), promoting coordinated control strategies supported by comprehensive source apportionment.

Emissions of reactive nitrogen species, particularly nitrogen oxides (NO_x) and ammonia (NH_3), play critical roles in $PM_{2.5}$ and O_3 formation. NH_3, mostly released from nitrogenous fertilizer use and livestock manure, reacts with acid forms of sulfur dioxide and NO_x to form secondary inorganic aerosols (Gu et al., 2021; Guo et al., 2024). Meanwhile, NO_x emissions from fossil fuel combustion additionally drive local O_3 production through photochemical reactions with volatile organic compounds (VOCs) (Atkinson, 2000). Given the complex atmospheric processes between sources and sinks governing $PM_{2.5}$ and O_3 formation, the relationship between precursor nitrogen emissions and secondary pollution levels demonstrates strong non-linearity (Ding et al., 2021; Clappier et al., 2021).

* Corresponding authors.
E-mail addresses: zhul3@sustech.edu.cn (L. Zhu), jingwei@pku.edu.cn (J. Wei).

https://doi.org/10.1016/j.envint.2026.110343
Received 12 February 2026; Received in revised form 7 May 2026; Accepted 29 May 2026
Available online 3 June 2026

Despite the great importance in air quality degradation, a research gap remains in linking nitrogen controls and health outcomes, particularly for regions experiencing concurrent $PM_{2.5}$–O_3 pollution. In this study, we comprehensively model the joint health effects of global $PM_{2.5}$–O_3 co-exposure based on a machine learning-based high-quality pollution dataset and a pollutant-specific stratified relative risk framework. On top of that, we quantify anthropogenic NO_x and NH_3 contributions to $PM_{2.5}$–O_3 co-pollutant health burden through sensitivity simulations using the GEOS-Chem chemical transport model (Bey et al., 2001). Our results demonstrate non-linear, region- and season-dependent nitrogen effects, providing a framework for optimizing reactive nitrogen mitigation strategies to maximize public health benefits.

2. Data and methods

2.1. Daily $PM_{2.5}$ and O_3 surface concentrations

We employ a machine learning framework based on the extremely randomized trees method (Geurts et al., 2006), a state-of-the-art tree-based ensemble learning algorithm, to estimate daily mean $PM_{2.5}$ concentrations and maximum daily 8-hour average O_3 concentrations. Building upon our previous research (Wei et al., 2022, 2023), this model integrates multiple-source data, including ground-based observations, satellite remote sensing products, meteorological and atmospheric composition reanalysis datasets, emission inventories, as well as geospatial information encompassing population density, economic indicators, land cover, and topographic features. The generated spatially continuous high-resolution (10 km) surface $PM_{2.5}$ and O_3 concentration datasets are consistent with global in situ observations, with coefficients of determination exceeding 0.89 and mean absolute errors below 5.8 μg m^{-3} (Liu et al., 2024a). These validation results confirm the reliability of our modeling framework in capturing the spatiotemporal distributions of $PM_{2.5}$ and O_3.

2.2. $PM_{2.5}$–O_3 co-pollutant health burden

We quantify the premature deaths attributable to short-term exposure to $PM_{2.5}$ or O_3 using a classic log-linear exposure-response function (GBD 2019 Risk Factors Collaborators, 2020) as:

$$M = \frac{I}{365}\sum_i P_i\left[1 - RR(\Omega_i)^{-1}\right], \quad (1)$$

where M denotes daily country- or region-level premature deaths attributable to air pollution, $I/365$ is the daily baseline mortality rate in 2019 (https://vizhub.healthdata.org/gbd-results), P_i represents the population in grid cell i (http://sedac.ciesin.columbia.edu/data/collection/gpw-v4), and $RR(\Omega_i)$ is the relative risk at exposure level Ω compared to the theoretical minimum-risk exposure level (TMREL).

To model the interaction between $PM_{2.5}$ and O_3, we apply the stratified RRs from the global time-series study by C. Liu et al. (2023), which employs a random-effects multilevel meta-analysis to examine their interactive effects on daily mortality. A total of 3 RR values are used for each pollutant (Table S1), with the cut-points for each grid defined by the first and third quartiles (i.e., 25th and 75th percentiles) of their daily concentrations (Figure S1). For comparative analysis between interactive and non-interactive scenarios, we use the unstratified RR values from C. Liu et al. (2023), which are 1.0079 (95% CI: 1.0066–1.0091) for individual $PM_{2.5}$ and 1.0031 (1.0025–1.0037) for individual O_3 with an increase in pollutant concentration per 10 μg m^{-3}. TMRELs range between 2.4 and 5.9 μg m^{-3} for $PM_{2.5}$ and 57.1 and 70.1 μg m^{-3} for O_3 (GBD 2019 Risk Factors Collaborators, 2020).

We propagate the uncertainty in the input to the mortality estimates with the Monte Carlo simulations (Xiao et al., 2021; Liu et al., 2024c). Baseline mortality rates and relative risk functions with 95% CI are modeled using normal distributions, while uncertainties in TMRELs are derived from uniform distribution. For exposure estimates, we apply normal distributions parameterized with cross-validation standard errors (0.024 μg m^{-3} for $PM_{2.5}$ and 0.013 μg m^{-3} for O_3). Through 2000 independent iterations that sampled from these probability distributions, we calculate mortality values using Eq. (1) with the central estimate represented by the mean of all simulations and the 95% CI determined from the empirical distribution.

2.3. Fractional sector impacts from NO_x and NH_3

Based on the zeroing-out method, we calculate fractional impacts F_i as the relative differences between a base simulation (including all emissions) and sensitivity simulations (excluding anthropogenic NO_x or NH_3 emissions). Hourly tracer concentrations from GEOS-Chem are aggregated into 24-hour mean $PM_{2.5}$ and maximum daily 8-hour average O_3 concentrations for each grid cell. Subsequently, population-weighted fractional source impacts F_{source} are quantified on a daily basis as:

$$F_{\text{source}} = \frac{\sum_i F_i \times \Omega_i \times P_i}{\sum_i P_i} \Big/ \frac{\sum_i \Omega_i \times P_i}{\sum_i P_i}, \quad (2)$$

with Ω_i and P_i respectively indicating the pollution concentration and population in i grid cell for each country. The monthly mean of these daily source contributions F_{source} is then multiplied by the monthly sum of the single-day health burden M from Eq. (1) to calculate the absolute contributions.

The base simulation and perturbation simulations in 2019 are implemented using the GEOS-Chem chemical transport model (http://www.geos-chem.org) with detailed O_3–NO_x-VOCs-halogens-aerosols chemistry (version 12.9.3). Driven by assimilated meteorological data from the Modern-Era Retrospective Analysis for Research and Applications, Version 2 (MERRA-2) (Gelaro et al., 2017), the global simulations are configured at a resolution of 2° × 2.5° with a spin-up time of 1 year. Anthropogenic emissions for 2019 are obtained from the Community Emissions Data System (CEDS) inventory (Hoesly et al., 2018). Soil NO_x emissions are estimated using the Berkeley Dalhousie Soil NO_x Parameterization (BDSNP) scheme (Hudman et al., 2012). Biogenic emissions are calculated using the Model of Emissions of Gases and Aerosols from Nature (MEGAN) version 2.1 (Guenther et al., 2012). Biomass burning emissions are sourced from the fourth-generation Global Fire Emissions Database (GFED4) (Giglio et al., 2013).

The GEOS-Chem model demonstrates robust performance in simulating spatial patterns of air pollutant concentrations, with a correlation coefficient of 0.75 and a relative mean bias of 30.4% for $PM_{2.5}$ and 0.77 and 38.7% for O_3, as evaluated against global in situ observations (Liu et al., 2024c). These biases are potentially related to uncertainties in anthropogenic and natural emission inventories, meteorological field representations, and parameterizations of key chemical processes (Fritz et al., 2022). Due to the use of relative differences in describing source contributions via the zero-out method, our method is less sensitive to the absolute biases in GEOS-Chem simulations, as analyzed in our previous works (S. Liu et al., 2023; Liu et al., 2024b). Nevertheless, we note that our results are likely most reliable for regions with dense monitoring networks and robust model validation, including East Asia, North America, and Europe, where the machine learning exposure dataset achieves higher accuracy and GEOS-Chem shows better performance.

3. Results and discussion

3.1. Global health burden of $PM_{2.5}$–O_3 co-exposure

In 2019, the interactive health effects of short-term $PM_{2.5}$ and O_3 exposure result in 1.46 (95% CI: 1.23–1.66) million premature deaths globally, with $PM_{2.5}$ accounting for 86.2% of the burden (Figure S2). This joint estimate is 24.8% higher than the sum of the non-interactive

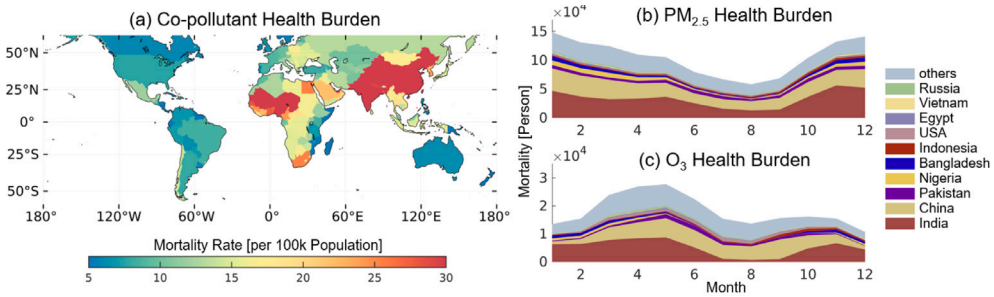

Fig. 1. Global health burden attributable to $PM_{2.5}$ and O_3 co-pollutant and monthly mortality from the top 10 countries in 2019.

individual pollutant effects (Figure S3), demonstrating significant synergistic interaction under co-exposure conditions (C. Liu et al., 2023). High co-pollutant mortality rates (up to 39.7 [95% CI: 34.0–44.3] per 100 thousand population) concentrate in Asian and Western African countries, followed by the Middle East and Southern Africa (Fig. 1). These high-risk regions are characterized by elevated concentrations of $PM_{2.5}$–O_3 co-pollutants (Figure S4), driven by intensive precursor emissions and unfavorable meteorological conditions, in line with previous studies (Chen et al., 2020; Lyu et al., 2023; He et al., 2024). We note that our non-interactive estimations are lower than those reported in the existing literature from Yu et al. (2024), which is likely attributable to our use of a log-linear exposure-response function, rather than the linear function they used.

India and China collectively account for 55.6% of the joint $PM_{2.5}$–O_3 mortality burden despite representing 36.9% of the population. In particular, India shows the most severe $PM_{2.5}$-attributable impacts, with November mortality reaching 47.5 (95% CI: 42.4–52.1) thousand deaths, due to agricultural burning emissions and atmospheric stagnation (Singh et al., 2023; Zhou et al., 2024), whereas China faces warm-season O_3 challenges (reaching 8.5 [4.6–10.4] thousand deaths in May) under intensified photochemical production. The health burden extends beyond these two nations, with 6 of the top 10 countries belonging to the Next Eleven (N-11) nations, including Pakistan, Nigeria, Bangladesh, Indonesia, Egypt, and Vietnam. Together, these nations witness 248.9 (95% CI: 213.2–279.0) thousand co-pollutant premature deaths annually, representing 17.0% of the global total. Given their rapid economic growth and delayed stringent air quality regulations, this health risk is projected to intensify in the coming decades.

3.2. $PM_{2.5}$–O_3 Co-pollutant health impacts driven by nitrogen emissions

Globally, 20.3% and 19.4% of the $PM_{2.5}$–O_3 co-pollutant-related deaths are attributable to anthropogenic NO_x and NH_3 emissions, respectively, though their relative importance varies regionally (Fig. 2). Industrializing and urbanizing nations reliant on fossil fuel-dependent energy infrastructure and heavy-duty diesel vehicles show elevated NO_x-related health effects. For instance, China, Saudi Arabia, and Malaysia witness up to 11.8 (95% CI: 10.1–13.2) deaths per 100 thousand population. Conversely, agricultural economies with intensive livestock production and fertilizer use, such as Poland, Mongolia, and Brazil, exhibit increased NH_3-associated health risks, with mortality rates reaching 1.7 (95% CI: 1.4–1.9) per 100 thousand population. A noteworthy finding concerns Asian nations, including Japan, South Korea, Nepal, and Thailand, which, while not listing on the highest co-pollutant health burden in Fig. 1, demonstrate severe nitrogen-related health impacts (Figure S5).

Beyond regional variations, the health impacts of NO_x and NH_3 also exhibit strong seasonal differences due to their distinct roles in the formation of $PM_{2.5}$ and O_3. Globally, the contributions of NH_3 to $PM_{2.5}$-related mortality are 29.5 to 56.9% greater than those from NO_x on a monthly basis (Figure S5). The NH_3-related health impacts peak during spring in China and post-monsoon periods in India, coinciding with intensive agricultural activities. NO_x, meanwhile, participates in $PM_{2.5}$ formation while simultaneously driving substantial O_3-related mortality , with the most severe burden during photochemically active warm seasons, such as summer months in China and pre-monsoon periods in India.

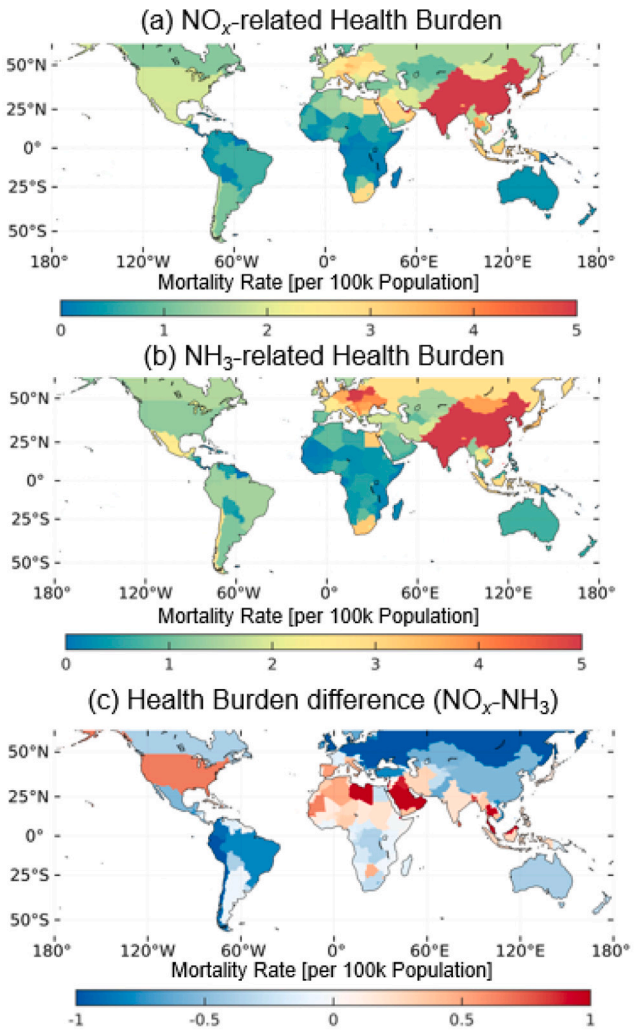

Fig. 2. Anthropogenic NO_x and NH_3 contributions to health burden attributable to $PM_{2.5}$–O_3 co-pollutant and their differences. Panel (a) shows the results from eliminating anthropogenic NO_x emissions while keeping NH_3 emissions at current baseline levels. Panel (b) shows the results from eliminating anthropogenic NH_3 emissions while keeping NO_x emissions at the predicted values.

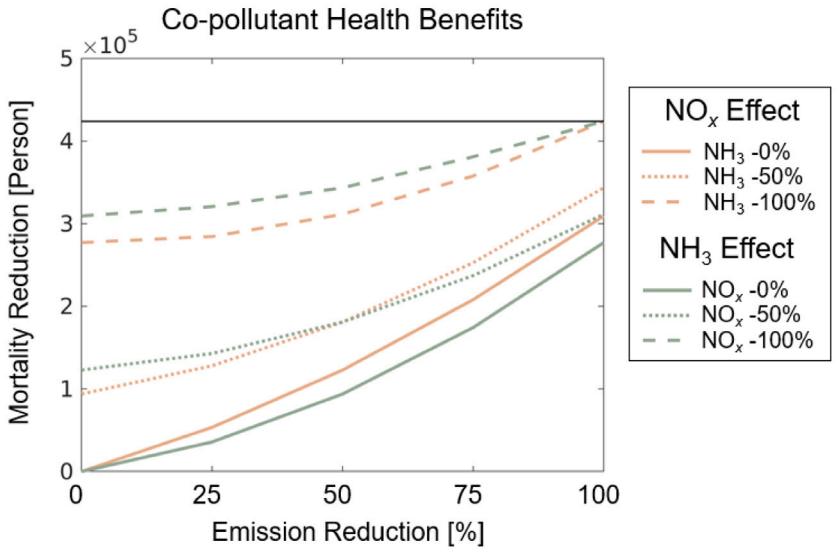

Fig. 3. Health benefits of $PM_{2.5}$–O_3 co-pollutant reductions through anthropogenic NO_x and NH_3 emission controls. Black horizontal lines show the health benefits from completely eliminating NO_x and NH_3 emissions. Brown lines show impacts of NO_x reduction under varying NH_3 phase-out levels (0%, 50%, and 100%). Green lines show effects of NH_3 reduction under varying NO_x phase-out levels. (For interpretation of the references to color in this figure legend, the reader is referred to the web version of this article.)

3.3. Non-linear effectiveness of nitrogen mitigation strategies

Effective development of mitigation strategies necessitates consideration of the intricate interaction between nitrogen emission reductions and associated health benefits (Fig. 3). NO_x reductions typically yield greater $PM_{2.5}$–O_3 co-pollutant health benefits compared to NH_3 mitigation. At current NH_3 emission levels (i.e., 0% NH_3 reduction), moderate 50% and deep 100% NO_x reductions respectively prevent 116.4 (95% CI: 96.7–133.2) and 283.9 (229.8–331.2) thousand premature deaths, surpassing equivalent NH_3 reductions under baseline NO_x conditions by 27.5% and 8.18%. The greatest health gains are achieved through complete NO_x abatement (i.e., 100% NO_x reduction) combined with progressive NH_3 controls. These co-pollutant effects reverse for $PM_{2.5}$-specific results (Figure S6), where NH_3 control proves more effective than NO_x reduction, consistent with findings from Guo et al. (2024).

The $PM_{2.5}$–O_3 co-pollutant health benefits from both NO_x and NH_3 reductions follow non-linear relationships with intervention intensity, with marginal gains increasing disproportionately under deeper emission cuts. For example, at current NH_3 levels, the first 50% NO_x reduction (from 0% to 50%) avoids only 39.9% of the total avoidable mortality reduction, whereas the final 50% cut (from 50% to 100%) contributes 60.1%. This non-linear behavior is even more pronounced for NH_3 under baseline NO_x conditions, where reducing emissions from 50% to 100% accounts for 66.2% of the total health gain. Notably, the degree of non-linearity intensifies as controls become more stringent for both nitrogen species. To illustrate, when background NH_3 emissions are reduced by 0%, 50%, and 100%, the deep NO_x reductions from 50% to 100% contribute 60.1%, 65.0%, and 76.9% of the total benefit, respectively.

The general non-linear effectiveness of nitrogen control strategies varies across regions and seasons (Fig. 4). Regionally, African regions exhibit relatively low responsiveness to anthropogenic nitrogen emissions despite substantial co-pollutant health burden, likely due to the strong natural contributions from mineral dust, biomass burning, and soil emissions (McDuffie et al., 2021). In contrast, densely populated South Asia, East Asia, and High Income Asia Pacific show greater mortality reduction potential, with either NO_x or NH_3 removal alone preventing more than 4.22 (95% CI: 3.57–4.78) mortality per 100k population annually. While additional 50% reductions in complementary NH_3 or NO_x further enhance these benefits, the health gains remain disproportionately smaller than those from full dual-gas mitigation, confirming the non-linear response in Fig. 3.

Seasonally, while NO_x emissions generally impose health burden equal or greater than that of NH_3 from March to August (up to 2.46 times), controlling NH_3 becomes more important than NO_x during the $PM_{2.5}$-dominant September–February for South Asia, East Asia, North Africa/Middle East, High Income Asia Pacific, and High Income North America, and Central Latin America (by a factor of 1.15 to 1.87). Particularly, in cold-season Europe, mitigating NH_3 alone delivers health benefits comparable to simultaneously eliminating both NO_x and NH_3. This phenomenon can be attributed to NH_3-limited nitrate formation under low-temperature conditions, where abundant NO_x saturates the nitric acid production pathway, while NH_3's lower molecular weight enables more efficient particulate nitrate reduction (Clappier et al., 2021).

3.4. Implication for nitrogen-related health management

Our work models the interactive health burden from $PM_{2.5}$–O_3 co-pollution and shows the complex roles of anthropogenic nitrogen control in public health management. The results reveal that $PM_{2.5}$–O_3 co-exposure causes 1.46 (95% CI: 1.23–1.66) million premature deaths globally, 24.8% greater than predictions by simple additive effects. This underscores the urgent need to revise air quality standards by accounting for synergistic interactions and implementing integrated precursor control strategies, especially in emerging economies that bear 72.6% of the global health burden.

Moreover, our work shows that anthropogenic NO_x and NH_3 emissions are responsible for 20.3% and 19.4%, respectively, of the $PM_{2.5}$–O_3 co-pollutant mortality burden, promoting season- and region-targeted fossil fuel combustion control and agricultural management. To effectively mitigate co-pollutant health impacts, a hypothetical removal of anthropogenic NO_x is 8.18% more effective than NH_3 control to achieve early gains, while simultaneous NO_x and NH_3 mitigation is essential for optimal long-term health benefits. Importantly, due to the non-linear relationship between emission reductions and health benefits, only aggressive emission cuts can generate proportionally

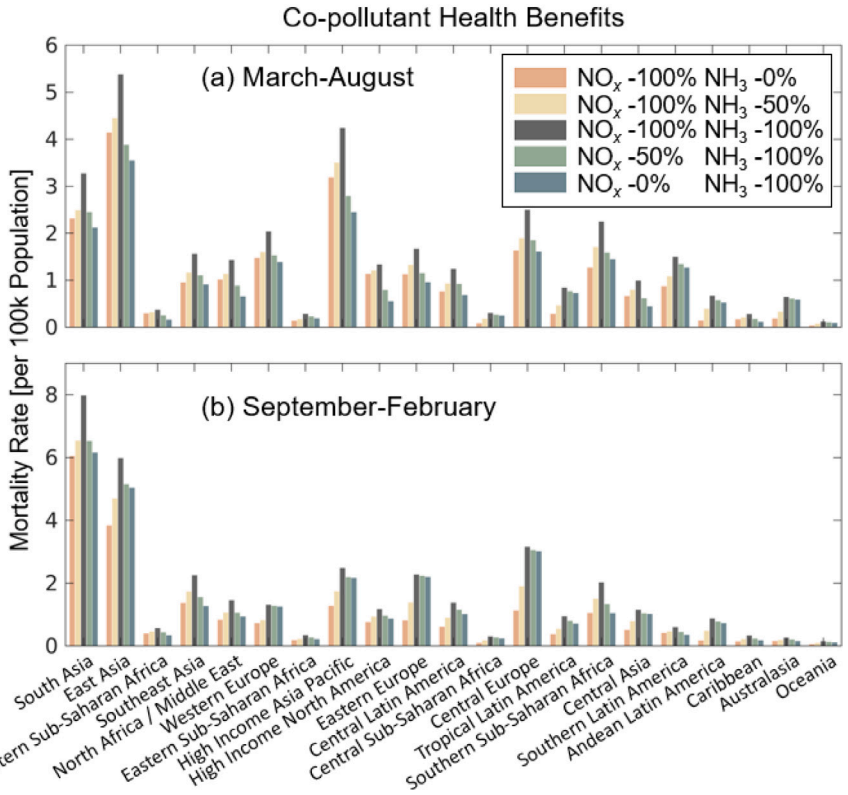

Fig. 4. Health benefits from reducing anthropogenic NO_x and NH_3 emissions. Reduction strategies include 100% NO_x and 0% NH_3 (i.e., eliminating NO_x and keeping current NH_3), 100% NO_x and 50% NH_3, 100% NO_x and 100% NH_3, 50% NO_x and 100% NH_3, and 0% NO_x and 100% NH_3. Regions are sorted based on total co-pollutant mortality rates. March–August defines the warm season for the Northern Hemisphere and the cold season for the Southern Hemisphere.

meaningful health gains, at least 20.2% more effective than mild control measures.

Despite substantial declines in anthropogenic NO_x emissions achieved through decades of worldwide clean air policies, these emissions remain a critical environmental and health concern due to their role in driving both $PM_{2.5}$ and O_3 formation, particularly in industrializing and urbanizing regions. Lessons and experiences show that end-of-pipe technologies tended be a cost-efficient way to control pollution in industries processes (Yan et al., 2023), whereas renewable energy application is more cost-effective in fossil fuel-related sectors, such as power plants, industry combustion, domestic combustion, and transportation (Zhang et al., 2020). These strategies hold relevance not just for air quality improvement in developing countries but also for global climate mitigation, as future carbon-neutral fuels could inadvertently increase nitrogen emissions without proper combustion optimization and post-combustion measures (F. Wang et al., 2021; Sher et al., 2025).

Given the projected growing global food demand and important role in cold-season $PM_{2.5}$ chemistry, NH_3 control appears as an increasingly necessary and attractive mitigation strategy, especially in light of cost-effectiveness and policy gaps (Gu et al., 2021). NH_3 mitigation strategies generally require optimizing synthetic fertilizer use and improving livestock manure management. Key practices for optimizing fertilization application and N use efficiency include deep placement of nitrogen fertilizers, substitution of synthetic fertilizer with (bio-)organic alternatives, and adoption of slow- or controlled-release fertilizers and nitrification inhibitors (Cheng et al., 2002; Hou et al., 2010; Geng et al., 2021; X. Wang et al., 2021; Pan et al., 2022). For livestock manure management, effective mitigation technologies and practices comprise lowering dietary crude protein and implementing solid–liquid separation during the housing stage, manure acidification and covering during manure storage and treatment stage, and proper spatial planning of livestock production (Hou et al., 2015; Wang et al., 2017; Bai et al., 2022; Yan et al., 2024).

The integration of the aforementioned NO_x and NH_3 mitigation practices is receiving growing attention in future air quality control initiatives. In Europe, the National Emission Ceilings Directive (2016/2284/EU) mandates a reduction of approximately 40% in NO_x and about 15% in NH_3 by 2030 compared to 2017 levels. The United States, under the Cross-State Air Pollution Rule Update, focuses primarily on the power sector, aiming to achieve a 20% reduction in NO_x emissions by 2030 relative to 2021. Meanwhile, China's 14th Five-Year Plan (2021–2025) and Long-Range Objectives Through the Year 2035 aims to cut NO_x emissions by over 10% by 2025 based on 2020 levels, while the Action Plan for Continuous Air Quality Improvement sets a target of reducing NH_3 emissions by 5% within the Beijing–Tianjin–Hebei region by 2025. However, the above-mentioned pace of implementation, progressing at annual reduction rates of approximately 2%–4% for NO_x and even slower for NH_3 (around 1%), significantly lack the ambition as well as urgency required to close the gap with effective health benchmarks identified in our study.

4. Uncertainties and limitations

This study is subject to several uncertainties and limitations. First, we acknowledge that the relative risk estimates used in this study (C. Liu et al., 2023) are mainly derived from cities in the northern hemisphere. Although this assumption is necessary in global burden assessments, applying these urban estimates to rural settings or regions with different climate conditions, socioeconomic status, or emission patterns may introduce bias. Second, our health burden estimates focus exclusively on the interactive effects of $PM_{2.5}$ and O_3, and thus the NO_x reduction scenarios presented in this study do not account for the additional direct health benefits associated with reduced NO_2 exposure.

Globally, short-term NO_2 exposure has been estimated to cause 198.2 (95% CI: 170.4–220.9) thousand premature deaths annually (Liu et al., 2024c). Therefore, the actual health benefits of NO_x mitigation are likely underestimated in our framework. Third, our health burden estimates are limited to premature mortality, without accounting for the broader health outcomes associated with $PM_{2.5}$ and O_3 exposure. Reductions in $PM_{2.5}$ and O_3 concentrations are expected to yield decreased morbidity from respiratory diseases and cardiovascular diseases (Shang et al., 2013; GBD 2021 Risk Factors Collaborators, 2024). Future work should integrate both mortality and morbidity outcomes to provide a more complete assessment of the public health gains from $PM_{2.5}$ and O_3 control strategies. Last, we acknowledge the mismatch in spatial resolution between exposure fields and source contributions and the assumption that source contributions are approximately constant within each month. To assess the robustness of our conclusions, we conduct sensitivity experiments by systematically varying the spatial and temporal resolutions of the exposure fields and source contributions (Table S2). As shown in Table S3, spatially aggregating the original 10 km exposure fields to 100 km and 200 km reduces the estimated interactive mortality from 24.8% to 22.0% and 21.4%, respectively, while nitrogen emission impacts vary by less than 2.2%. Temporally, using weekly or bi-weekly aggregations yields unchanged results. These sensitivity tests confirm that our main findings are robust despite these acknowledged limitations.

CRediT authorship contribution statement

Song Liu: Writing – original draft, Methodology, Formal analysis, Conceptualization. **Xicheng Li:** Writing – review & editing, Software, Resources, Conceptualization. **Lei Shu:** Writing – review & editing, Visualization. **Tzung-May Fu:** Writing – review & editing, Supervision. **Xin Yang:** Writing – review & editing, Supervision. **Lei Zhu:** Writing – original draft, Formal analysis, Conceptualization. **Jing Wei:** Writing – original draft, Resources, Methodology, Data curation.

Declaration of competing interest

The authors declare that they have no known competing financial interests or personal relationships that could have appeared to influence the work reported in this paper.

Acknowledgments

This work is funded by Jing-Jin-Ji Regional Integrated Environmental Improvement-National Science and Technology Major Project (2026ZD1212900), National Natural Science Foundation of China (42575139), Guangdong Basic and Applied Basic Research Foundation (2024A1515011951), Guangdong Provincial Field Observation and Research Station for Coastal Atmosphere and Climate of the Greater Bay Area (2021B1212050024), Shenzhen Science and Technology Program (KQTD20210811090048025), High-level University Special Fund (G030290001), Fundamental and Interdisciplinary Disciplines Breakthrough Plan of the Ministry of Education of China (JYB2025XDXM906), National Key Technology and Development Program of Corps (2025AA001), and Fundamental Research Funds for the Central Universities, Peking University. This work is supported by the Center for Computational Science and Engineering at the Southern University of Science and Technology.

Appendix A. Supplementary data

Supplementary material related to this article can be found online at https://doi.org/10.1016/j.envint.2026.110343.

Data availability

Data will be made available on request.

References

Atkinson, R., 2000. Atmospheric chemistry of VOCs and NO_x. Atmos. Environ. 34 (12–14), 2063–2101.

Bai, Z., Fan, X., Jin, X., Zhao, Z., Wu, Y., Oenema, O., Velthof, G., Hu, C., Ma, L., 2022. Relocate 10 billion livestock to reduce harmful nitrogen pollution exposure for 90% of China's population. Nat. Food 3, 152–160.

Bey, I., Jacob, D.J., Yantosca, R.M., Logan, J.A., Field, B.D., Fiore, A.M., Li, Q., Liu, H.Y., Mickley, L.J., Schultz, M.G., 2001. Global modeling of tropospheric chemistry with assimilated meteorology: Model description and evaluation. J. Geophys. Res.: Atmospheres 106 (D19), 23073–23095.

Chen, Y., Wild, O., Ryan, E., Sahu, S.K., Lowe, D., Archer-Nicholls, S., Wang, Y., McFiggans, G., Ansari, T., Singh, V., Sokhi, R.S., Archibald, A., Beig, G., 2020. Mitigation of $PM_{2.5}$ and ozone pollution in Delhi: a sensitivity study during the pre-monsoon period. Atmos. Chem. Phys. 20, 499–514.

Cheng, W., Nakajima, Y., Sudo, S., Akiyama, H., Tsuruta, H., 2002. N_2O and NO emissions from a field of Chinese cabbage as influenced by band application of urea or controlled-release urea fertilizers. Nutr. Cycl. Agroecosystems 63, 231–238.

Clappier, A., Thunis, P., Beekmann, M., Putaud, J., De Meij, A., 2021. Impact of SO_x, NO_x and NH_3 emission reductions on $PM_{2.5}$ concentrations across Europe: Hints for future measure development. Environ. Int. 156, 106699.

Ding, D., Xing, J., Wang, S., Dong, Z., Zhang, F., Liu, S., Hao, J., 2021. Optimization of a NO_x and VOC cooperative control strategy based on clean air benefits. Environ. Sci. Technol. 56, 739–749.

Fritz, T.M., Eastham, S.D., Emmons, L.K., Lin, H., Lundgren, E.W., Goldhaber, S., Barrett, S.R.H., Jacob, D.J., 2022. Implementation and evaluation of the GEOS-chem chemistry module version 13.1.2 within the community earth system model v2.1. Geosci. Model. Dev. 15 (23), 8669–8704.

GBD 2019 Risk Factors Collaborators, 2020. Global burden of 87 risk factors in 204 countries and territories, 1990–2019: a systematic analysis for the global burden of disease study 2019. Lancet 396 (10258), 1223–1249.

GBD 2021 Risk Factors Collaborators, 2024. Global burden and strength of evidence for 88 risk factors in 204 countries and 811 subnational locations, 1990–2021: a systematic analysis for the global burden of disease study 2021. Lancet 403 (10440), 2162–2203.

Gelaro, R., McCarty, W., Suárez, M.J., Todling, R., Molod, A., Takacs, L., Randles, C.A., Darmenov, A., Bosilovich, M.G., Reichle, R., Wargan, K., Coy, L., Cullather, R., Draper, C., Akella, S., Buchard, V., Conaty, A., da Silva, A.M., Gu, W., Kim, G.-K., Koster, R., Lucchesi, R., Merkova, D., Nielsen, J.E., Partyka, G., Pawson, S., Putman, W., Rienecker, M., Schubert, S.D., Sienkiewicz, M., Zhao, B., 2017. The modern-era retrospective analysis for research and applications, version 2 (MERRA-2). J. Clim. 30 (14), 5419–5454.

Geng, Y., Yuan, Y., Miao, Y., Zhi, J., Huang, M., Zhang, Y., Wang, H., Shen, Q., Zou, J., Li, S., 2021. Decreased nitrous oxide emissions associated with functional microbial genes under bio-organic fertilizer application in vegetable fields. Pedosphere 31 (2), 279–288.

Geurts, P., Ernst, D., Wehenkel, L., 2006. Extremely randomized trees. Mach. Learn. 63, 3–42.

Giglio, L., Randerson, J.T., Van Der Werf, G.R., 2013. Analysis of daily, monthly, and annual burned area using the fourth-generation global fire emissions database (GFED4). J. Geophys. Res.: Biogeosciences 118 (1), 317–328.

Gu, B., Zhang, L., Van Dingenen, R., Vieno, M., Van Grinsven, H.J., Zhang, X., Zhang, S., Chen, Y., Wang, S., Ren, C., Rao, S., Holland, M., Winiwarter, W., Chen, D., Xu, J., Sutton, M.A., 2021. Abating ammonia is more cost-effective than nitrogen oxides for mitigating $PM_{2.5}$ air pollution. Science 374, 758–762.

Guenther, A., Jiang, X., Heald, C.L., Sakulyanontvittaya, T., Duhl, T., Emmons, L., Wang, X., 2012. The model of emissions of gases and aerosols from nature version 2.1 (MEGAN2.1): an extended and updated framework for modeling biogenic emissions. Geosci. Model. Dev. 5 (6), 1471–1492.

Guo, Y., Zhang, L., Winiwarter, W., van Grinsven, H.J., Wang, X., Li, K., Pan, D., Liu, Z., Gu, B., 2024. Ambitious nitrogen abatement is required to mitigate future global $PM_{2.5}$ air pollution toward the World Health Organization targets. One Earth 7, 1600–1613.

He, C., Liu, J., Zhou, Y., Zhou, J., Zhang, L., Wang, Y., Liu, L., Peng, S., 2024. Synergistic $PM_{2.5}$ and O_3 control to address the emerging global $PM_{2.5}$-O_3 compound pollution challenges. Eco-Environ. Health 3, 325–337.

Hoesly, R.M., Smith, S.J., Feng, L., Klimont, Z., Janssens-Maenhout, G., Pitkanen, T., Seibert, J.J., Vu, L., Andres, R.J., Bolt, R.M., Bond, T.C., Dawidowski, L., Kholod, N., Kurokawa, J.-I., Li, M., Liu, L., Lu, Z., Moura, M.C.P., O'Rourke, P.R., Zhang, Q., 2018. Historical (1750–2014) anthropogenic emissions of reactive gases and aerosols from the Community Emissions Data System (CEDS). Geosci. Model. Dev. 11 (1), 369–408.

Hou, A., Tsuruta, H., McCreary, M.A., Hosen, Y., 2010. Effect of urea placement on the time-depth profiles of NO, N_2O and mineral nitrogen concentrations in an andisol during a Chinese cabbage growing season. Soil Sci. Plant Nutr. 56 (6), 861–869.

Hou, Y., Velthof, G.L., Oenema, O., 2015. Mitigation of ammonia, nitrous oxide and methane emissions from manure management chains: a meta-analysis and integrated assessment. Global Change Biol. 21, 1293–1312.

Hudman, R., Moore, N., Mebust, A., Martin, R., Russell, A., Valin, L., Cohen, R., 2012. Steps towards a mechanistic model of global soil nitric oxide emissions: implementation and space based-constraints. Atmos. Chem. Phys. 12 (16), 7779–7795.

Liu, C., Chen, R., Sera, F., Vicedo-Cabrera, A.M., Guo, Y., Tong, S., Lavigne, E., Correa, P.M., Ortega, N.V., Achilleos, S., Roye, D., Jaakkola, J.J.K., Ryti, N., Pascal, M., Schneider, A., Breitner, S., Entezari, A., Mayvaneh, F., Raz, R., Honda, Y., Hashizume, M., Ng, C.F.S., Gaio, V., Madureira, J., Holobaca, I.H., Tobias, A., Iniguez, C., Guo, Y.L., Pan, S.C., Masselot, P., Bell, M.L., Zanobetti, A., Schwartz, J., Gasparrini, A., Kan, H., 2023. Interactive effects of ambient fine particulate matter and ozone on daily mortality in 372 cities: two stage time series analysis. BMJ 383, e075203.

Liu, S., Li, X., Li, J., Shu, L., Fu, T.-M., Yang, X., Zhu, L., 2023. Observing network effect of shipping emissions from space: A natural experiment in the world's busiest port. PNAS Nexus 2 (11), pgad391. http://dx.doi.org/10.1093/pnasnexus/pgad391.

Liu, S., Li, X., Wei, J., Shu, L., Jin, J., Fu, T.-M., Yang, X., Zhu, L., 2024a. Short-term exposure to fine particulate matter and ozone: Source impacts and attributable mortalities. Environ. Sci. Technol. 58 (26), 11256–11267.

Liu, S., Shu, L., Zhu, L., Song, Y., Sun, W., Chen, Y., Wang, D., Pu, D., Li, X., Sun, S., Li, J., Zuo, X., Fu, W., Yang, X., Fu, T.-M., 2024b. Underappreciated emission spikes from power plants during heatwaves observed from space: Case studies in India and China. Earth's Future 12 (1), e2023EF003937. http://dx.doi.org/10.1029/2023EF003937.

Liu, S., Wei, J., Li, X., Shu, L., Zhang, J., Fu, T.-M., Yang, X., Zhu, L., 2024c. Underappreciated roles of soil nitrogen oxide emissions on global acute health burden. Environ. Int. 193, 109087.

Lyu, X., Li, K., Guo, H., Morawska, L., Zhou, B., Zeren, Y., Jiang, F., Chen, C., Goldstein, A.H., Xu, X., Wang, T., Lu, X., Zhu, T., Querol, X., Chatani, S., Latif, M.T., Schuch, D., Sinha, V., Kumar, P., Mullins, B., Seguel, R., Shao, M., Xue, L., Wang, N., Chen, J., Gao, J., Chai, F., Simpson, I., Sinha, B., Blake, D.R., 2023. A synergistic ozone-climate control to address emerging ozone pollution challenges. One Earth 6 (8), 964–977.

McDuffie, E.E., Martin, R.V., Spadaro, J.V., Burnett, R., Smith, S.J., O'Rourke, P., Hammer, M.S., van Donkelaar, A., Bindle, L., Shah, V., Jaeglé, L., Luo, G., Yu, F., Adeniran, J.A., Lin, J., Brauer, M., 2021. Source sector and fuel contributions to ambient $PM_{2.5}$ and attributable mortality across multiple spatial scales. Nat. Commun. 12 (1), 3594.

Pan, S.-Y., He, K.-H., Lin, K.-T., Fan, C., Chang, C.-T., 2022. Addressing nitrogenous gases from croplands toward low-emission agriculture. Npj Clim. Atmos. Sci. 5 (1), 43.

Shang, Y., Sun, Z., Cao, J., Wang, X., Zhong, L., Bi, X., Li, H., Liu, W., Zhu, T., Huang, W., 2013. Systematic review of Chinese studies of short-term exposure to air pollution and daily mortality. Environ. Int. 54, 100–111.

Sher, F., Hameed, S., Omerbegovic, N.S., Wang, B., Hai, I.U., Rashid, T., Teoh, Y.H., Yildiz, M.J., 2025. Bioenergy with carbon capture and storage technology to achieve net zero emissions: A review. Renew. Sustain. Energy Rev. 210, 115229.

Singh, T., Matsumi, Y., Nakayama, T., Hayashida, S., Patra, P.K., Yasutomi, N., Kajino, M., Yamaji, K., Khatri, P., Takigawa, M., Araki, H., Kurogi, Y., Kuji, M., Muramatsu, K., Imasu, R., Ananda, A., Arbain, A.A., Ravindra, K., Bhardwaj, S., Kumar, S., Mor, S., Dhaka, S.K., Dimri, A.P., Sharma, A., Singh, N., Bhatti, M.S., Yadav, R., Vatta, K., 2023. Very high particulate pollution over northwest India captured by a high-density in situ sensor network. Sci. Rep. 13, 13201.

Wang, X., Bai, J., Xie, T., Wang, W., Zhang, G., Yin, S., Wang, D., 2021. Effects of biological nitrification inhibitors on nitrogen use efficiency and greenhouse gas emissions in agricultural soils: A review. Ecotoxicol. Environ. Safety 220, 112338.

Wang, Y., Dong, H., Zhu, Z., Gerber, P.J., Xin, H., Smith, P., Opio, C., Steinfeld, H., Chadwick, D., 2017. Mitigating greenhouse gas and ammonia emissions from swine manure management: a system analysis. Environ. Sci. Technol. 51, 4503–4511.

Wang, F., Harindintwali, J.D., Yuan, Z., Wang, M., Wang, F., Li, S., Yin, Z., Huang, L., Fu, Y., Li, L., Chang, S.X., Zhang, L., Rinklebe, J., Yuan, Z., Zhu, Q., Xiang, L., Tsang, D.C., Xu, L., Jiang, X., Liu, J., Wei, N., Kastner, M., Zou, Y., Ok, Y.S., Shen, J., Peng, D., Zhang, W., Barcelo, D., Zhou, Y., Bai, Z., Li, B., Zhang, B., Wei, K., Cao, H., Tan, Z., Zhao, L., He, X., Zheng, J., Bolan, N., Liu, X., Huang, C., Dietmann, S., Luo, M., Sun, N., Gong, J., Gong, Y., Brahushi, F., Zhang, T., Xiao, C., Li, X., Chen, W., Jiao, N., Lehmann, J., Zhu, Y.-G., Jin, H., Schaffer, A., Tiedje, J.M., Chen, J.M., 2021. Technologies and perspectives for achieving carbon neutrality. Innov. 2.

Wei, J., Li, Z., Li, K., Dickerson, R.R., Pinker, R.T., Wang, J., Liu, X., Sun, L., Xue, W., Cribb, M., 2022. Full-coverage mapping and spatiotemporal variations of ground-level ozone (O_3) pollution from 2013 to 2020 across China. Remote Sens. Environ. 270, 112775.

Wei, J., Li, Z., Lyapustin, A., Wang, J., Dubovik, O., Schwartz, J., Sun, L., Li, C., Liu, S., Zhu, T., 2023. First close insight into global daily gapless 1 km $PM_{2.5}$ pollution, driving factors, and health impact. Nat. Commun. 14 (1), 8349.

Xiao, Q., Geng, G., Xue, T., Liu, S., Cai, C., He, K., Zhang, Q., 2021. Tracking $PM_{2.5}$ and O_3 pollution and the related health burden in China 2013–2020. Environ. Sci. Technol. 56 (11), 6922–6932.

Yan, X., Xu, Y., Pan, G., 2023. Evolution of China's NO_x emission control strategy during 2005–2020 over coal-fired power plants: A satellite-based assessment. J. Environ. Manag. 348, 119243.

Yan, X., Ying, Y., Li, K., Zhang, Q., Wang, K., 2024. A review of mitigation technologies and management strategies for greenhouse gas and air pollutant emissions in livestock production. J. Environ. Manag. 352, 120028.

Yu, W., Xu, R., Ye, T., Abramson, M.J., Morawska, L., Jalaludin, B., Johnston, F.H., Henderson, S.B., Knibbs, L.D., Morgan, G.G., Lavigne, E., Heyworth, J., Hales, S., Marks, G.B., Woodward, A., Bell, M.L., Samet, J.M., Song, J., Li, S., Guo, Y., 2024. Estimates of global mortality burden associated with short-term exposure to fine particulate matter ($PM_{2.5}$). Lancet Planet. Health 8 (3), e146–e155. http://dx.doi.org/10.1016/S2542-5196(24)00003-2.

Zhang, F., Xing, J., Zhou, Y., Wang, S., Zhao, B., Zheng, H., Zhao, X., Chang, H., Jang, C., Zhu, Y., Hao, J., 2020. Estimation of abatement potentials and costs of air pollution emissions in China. J. Environ. Manag. 260, 110069.

Zhou, M., Xie, Y., Wang, C., Shen, L., Mauzerall, D.L., 2024. Impacts of current and climate induced changes in atmospheric stagnation on Indian surface $PM_{2.5}$ pollution. Nat. Commun. 15, 7448.